

# Bimodular behaviour and crack closure in compression in a brittle material

L. A. FELDMAN

*Materials Sciences Laboratory, The Aerospace Corporation, El Segundo, California 90245, USA*

A vibrating beam method was used to determine the elastic modulus of graphite rods. The frequency and apparent modulus were determined as a function of compressive end-loading. Following fracture of the rod, the frequency and apparent modulus were decreased. At a compressive end-loading of about 0.83 MPa (120 p.s.i.), crack closure was sufficient for the fractured rod to behave similarly in vibration to the unfractured rod. Thus, the fractured material behaves in a bimodular fashion and crack closure can be achieved to enable unimpeded stress transfer across the fracture surface during vibration.

## 1. Introduction

The presence of cracks in brittle materials can have a significant effect on the measured elastic properties. Numerous studies have investigated this effect experimentally in rock [1], graphite [2] and ceramics [3]; the effect has also been studied from a purely theoretical viewpoint [4]. Resonance techniques have been used to measure elastic properties in materials containing microcracks [3, 5]. Such macroscopically measured properties have sometimes been used to replace certain microscopic quantities [3], such as mean microcrack radius,  $\langle a \rangle$ , and number density of microcracks,  $N$ , which are difficult to determine experimentally.

In this experiment, the effect on the apparent elastic modulus of a single large crack, consisting of a complete fracture through the sample, was determined under compressive loading across the fracture surface. Sonic resonance was used because it can detect the change in modulus due to a single known and observable crack.

## 2. Experimental procedure

The experiment measured the sonic resonance of a simply supported, axially loaded thin beam of graphite. The material was a 3.2 mm (0.125 in) diameter, high-purity carbon spectrograph rod of bulk density  $1.58 \times 10^{-3} \text{ kg m}^{-3}$  ( $1.58 \text{ g cm}^{-3}$ ), apparent density (flotation method)  $1.93 \times 10^{-3} \text{ kg m}^{-3}$  ( $1.93 \text{ g cm}^{-3}$ ), and porosity 18 vol %. The sonic resonance method is similar in principle to methods described elsewhere [6, 7]. The beam was supported by sharply pointed metal contacts in the centres of the end faces.

Resonance was excited by placing the sample in the field of a cobalt-samarium permanent magnet and passing an a.c. current through the sample. The Lorentz force on the sample produces an oscillating force perpendicular to the magnetic field and the direction of current flow. The sample was observed with a binocular microscope. The frequency was varied until the resonance peak was observed; the

peak is easily visible as a smearing into a line of a point viewed on the sample. The resonance frequency could be located repeatedly to a precision of better than 1% each time. Stroboscopic illumination was occasionally used to freeze the sample motion to verify that the resonance was the fundamental transverse vibrational mode.

The sample was mounted vertically between the current-carrying point contacts at the ends (Fig. 1), and the top contact was mounted on a flexible support to which weights could be added so that the sample could be axially loaded during vibration. Resonance frequency, which was measured as a function of end loading, decreased with increasing load. The load was restricted to less than approximately one-half the Euler critical buckling load,  $P_b$ , to avoid breaking the sample.

The frequency against load was measured on the same sample, both as-machined and then after fracture at the midpoint. The 3.2 mm (0.125 in) diameter graphite rod, which was 40 mm long, was machined with a single edge notch at the midpoint, 0.2 mm wide and 0.2 mm deep, aligned perpendicular to the sample axis, to facilitate subsequent fracture at that location. A small piece of adhesive tape, about 1 mm  $\times$  4 mm, was placed on the sample to aid in maintaining orientation of the two faces after fracture. The tape had a negligible effect on the measured frequency, because its mass was small and its modulus low compared with those of the graphite rod.

After a number of measurements of frequency against load were taken on the sample, the rod was carefully and completely fractured through at the notch. The fractured ends were then mated together, the sample was replaced in the holder, and another series of frequency against load measurements was made. The fracture faces were photographed stereographically in the scanning electron microscope (SEM) to observe the degree of matching of the fracture faces.

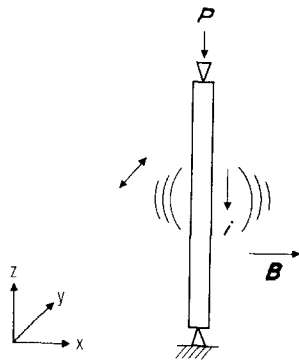


Figure 1 Schematic diagram of sonic resonance experiment:  $P$  = load,  $i$  = current,  $B$  = magnetic field. Arrows show direction of vibration in and out of the plane of the figure.

### 3. Theory

#### 3.1. Simply supported beam with axial loading

According to the theory of simple vibrating beams [8], a beam of length  $L$  supported at each end such that at the ends the displacements and the bending moments are zero (both  $y = 0$  and  $y'' = 0$  at  $x = 0$  and  $x = L$ ) has a frequency in the lowest mode of

$$f_0 = \frac{1}{2L} P_b^{1/2} (\rho A)^{-1/2} \quad (1)$$

where  $P_b$  is the Euler buckling load,  $\rho$  is the bulk mass density and  $A$  is the cross-sectional area. The term  $P_b$  is expressed as

$$P_b = \frac{\pi^2 EI}{L^2} \quad (2)$$

where  $E$  is Young's modulus and  $I$  is the moment of inertia of the cross-section.

If an axial compressive load,  $P$ , is imposed on the beam at the supports, the frequency of the lowest transverse vibrational mode becomes [8]

$$f = f_0 (1 - P/P_b)^{1/2} \quad (3)$$

where  $f_0$  (frequency of the unloaded beam) is given in Equation 1. In the graph of the behaviour of  $f$  against  $P$  (Fig. 2), as  $P$  approaches  $P_b$  the frequency approaches zero, which is to be expected since the beam is unstable with respect to a small transverse deflection at the buckling load, since the restoring force approaches zero. This relation between axial load, frequency and modulus can be used in analysing the experiment being discussed.

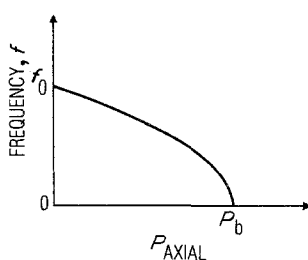


Figure 2 Frequency against axial load:  $f = f_0 (1 - P/P_b)^{1/2}$ .

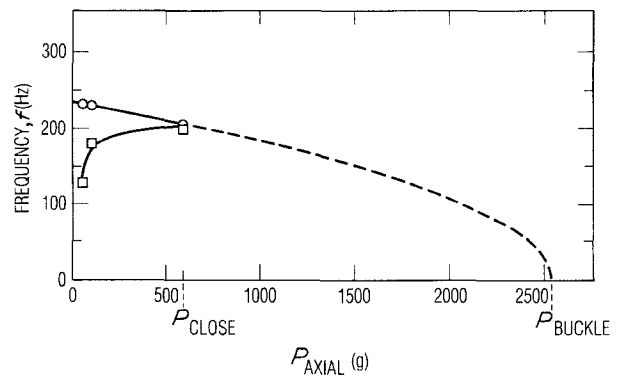


Figure 3 Frequency against axial load for sample (O) before and (□) after fracture.

#### 3.2. Axially loaded beam with cracks

Next we consider the effect of cracks on the vibrational behaviour of an axially loaded beam. Assuming a number of thin planar cracks in the material, all oriented perpendicular to the beam axis, we expect the stiffness of the beam in bending to be less than that for an uncracked beam. The rationale is that, whereas cracks might close on the compression side of the neutral axis, they would remain open on the tension side and hence no stress transfer would occur across the crack faces. Crack closure would make the material bimodular, with a higher Young's modulus in compression than in tension. If cracks did not become closed on the compression side, because the strains generated during bending were small compared with the crack-opening displacement, no bimodular effect on the apparent stiffness would be evidenced.

Changes in vibrational frequency are expected for an axially loaded beam, because the effective modulus would be higher than in the relaxed state, if the stress in the material created by the axial load were sufficient to close the cracks. During small vibrations, the cracks could remain closed, provided that the maximum tensile stress created by bending remained smaller than the compressive stress caused by the axial load. The beam would effectively be prestressed and would everywhere remain under residual compression in the axial direction.

If such crack closure were to occur at some level of axial loading, then Equation 3 would no longer hold as originally stated, because  $P_b$ , and hence  $f_0$ , would depend on  $P$ , since  $E$  would change with  $P$ . A simple system that illustrates this behaviour, consisting of a beam with many small annular cracks in the surface, is discussed in the Appendix.

### 4. Results and discussion

The experiment described above can be discussed in terms of the concepts of crack closure with increased stress transfer during loading. Fig. 3 plots the results of the frequency against load experiment for the same specimen, uncracked and cracked. While  $f$  decreased with increasing load in the uncracked case up to a load of about one-fourth the extrapolated buckling load, the sample after fracture behaved the opposite: near zero load,  $f_0$  (cracked) was about 50% of  $f_0$  (uncracked); as load was applied to the cracked sample, frequency

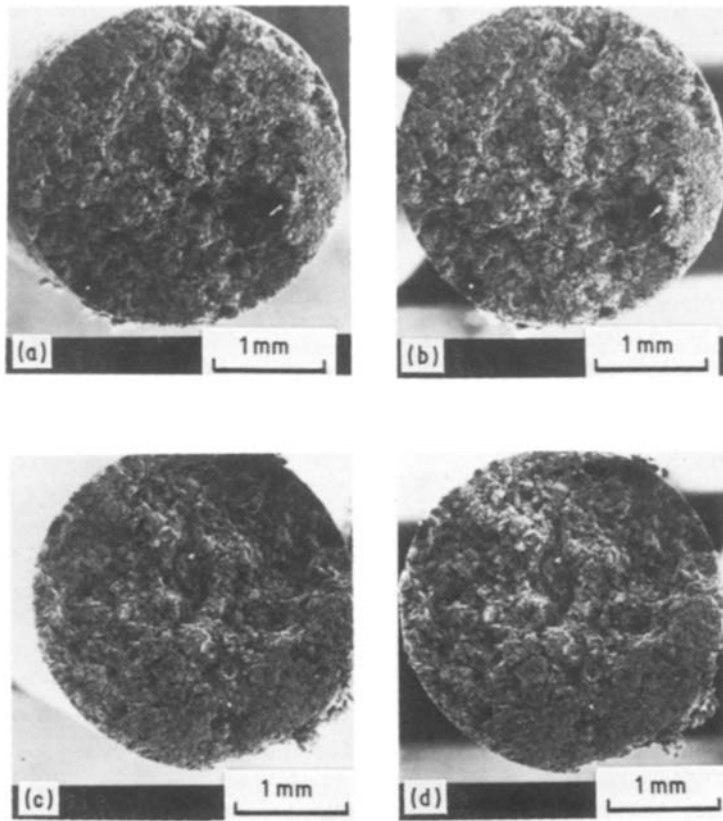


Figure 4 Stereomicrographs of fracture surfaces: (a, b) top surface, (c, d) bottom surface.

initially increased; and at  $P$  of about 25% of  $P_0$  of the uncracked specimen, the frequencies for both the cracked and uncracked samples were approximately the same, indicating that stress transfer across the crack faces was similar to that in unbroken material. The transfer occurs at an equivalent stress of about 0.83 MPa (120 p.s.i.), based on the cross-sectional area of the rod.

SEM stereographic pairs of the fracture surfaces of the graphite rod (Fig. 4) depict both surfaces as having a high degree of surface roughness and matching well (hills and valleys occur in corresponding locations). Yet when the surfaces are initially placed in contact, under small load, the load is not transferred uniformly across the interface, as indicated by the frequency, which is lower than that of the unbroken sample. Only after the load has reached a certain level does the frequency of the cracked sample become indistinguishable from that of the uncracked one. Although well matched initially, the fracture faces sustain enough damage or distortion to prevent them from seating together sufficiently for uniform stress transfer below a particular load. Once that load across the crack faces is achieved, the sample behaves elastically, as if the crack were not present, because the fracture faces remain in net compressive loading throughout the full vibrational cycle. This also shows that surface roughness of a crack is, in addition to the elastic behaviour of the unbroken material surrounding the crack, an important factor in crack reclosure.

As a final observation, graphite is an ideal material for this experiment, because it combines high electrical conductivity and brittle fracture. Non-conductive brittle materials can also be made to resonate by

applying a thin conductive stripe, such as metal film or conductive paint, along the specimen.

## 5. Conclusion

This experiment demonstrated that the presence of a simple fracture surface perpendicular to the beam axis in a graphite beam lowers its apparent modulus in sonic resonance. At a critical compressive stress, however, the fracture faces are brought back into contact sufficiently to transfer stress uniformly, so that the beam frequency approaches that of the unbroken state. Thus, the crack closure depends to some extent on surface roughness and on elastic properties, but sufficient registry of the faces can be achieved under compression to transfer the load uniformly across the fracture interface and maintain the faces in contact during vibration.

## Acknowledgements

The author thanks D. J. Chang, A. B. Chase, P. I. Gold, R. A. Meyer, M. A. Piliavin and F. D. Ross for helpful discussions. This work was supported in part by the Office of Naval Research.

## Appendix: Example of frequency dependence on axial load of a beam containing cracks

This Appendix presents a simple example of how the frequency of an axially loaded beam can be modified by changes in stiffness caused by crack closure. We assume a cylindrical beam of material of length  $L$ , radius  $r_1$ , and uncracked modulus  $E$ , and a set of  $N$  regularly spaced annular cracks in the outer surface of the beam (Fig. A1). The cracks have outer radius  $r_1$ ,

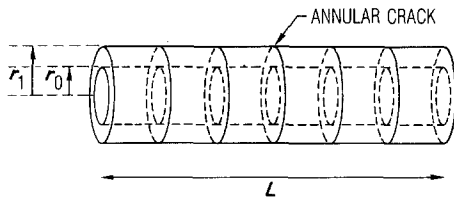


Figure A1 Cylindrical beam with annular cracks.

inner radius  $r_0$  and maximum crack opening displacement  $d$ , where  $Nd \ll L$ . At a certain axial load,  $P_c$ , the cracks close significantly. At the same time, since  $Nd \ll L$ , the overall length change of the sample can be ignored as a first approximation. The sample bulk density  $\rho$  is related to the sample mass  $M$  and cross-sectional area  $A$ , where  $A = \pi r_1^2$ , and is given by  $\rho = M/AL$ . The change in density under loading and crack closure is also ignored as a first approximation.

### A.1. Frequency against load—cracks open

The frequency against load for the material can now be calculated based on the properties for small vibrations at small loading,  $P < P_c$ , when the cracks remain open, and assuming that the crack spacing,  $L/N$ , is less than the width of the annulus,  $(r_1 - r_0)$ . In this case, the beam consists of an undamaged core of radius  $r_0$  and an outer shell of cracked material that carries essentially no tensile or compressive load and serves as dead weight [9]. From Equations 1 and 3

$$f_0 = \frac{1}{2L} P_b^{1/2} (\rho A)^{-1/2} \quad (\text{A1})$$

$$f = f_0 (1 - P/P_b)^{1/2} \quad P < P_c \quad (\text{A2})$$

where  $P_b = \pi^2 EI/L^2$  and  $I = \pi r_0^4/4$ .

### A.2. Frequency against load—cracks closed

The same relations for the beam when  $P$  is greater than  $P_c$  and the cracks are effectively closed by the axial load, and remain closed during small vibrations, are calculated from Equations 1 and 3 as

$$f'_0 = \frac{1}{2L} (P'_b)^{1/2} (\rho A)^{-1/2} \quad (\text{A3})$$

$$f' = f'_0 (1 - P/P'_b)^{1/2} \quad P > P_c \quad (\text{A4})$$

where  $P'_b = \pi^2 EI'/L^2$  and  $I' = \pi r_1^4/4$ .

Two  $f$  against  $P$  curves are predicted, in Fig. A2, one for the material with open cracks (from Equation A2) and one for closed cracks (from Equation A4). In

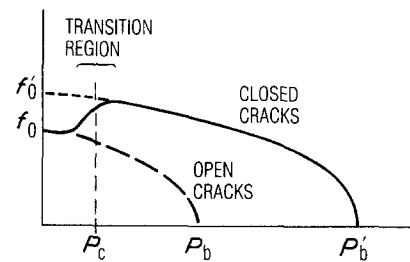


Figure A2 Crack closure under load and change of  $f_0$  and  $P_b$ .

a realizable material, crack closure would be expected to be gradual over some load range, rather than abrupt at an exact loading  $P_c$ ; therefore, a positive deviation from the  $f$  against  $P$  curve would be expected for the cracked material as load is applied, eventually meeting the curve for the closed-crack material beyond  $P_c$ . For this reason, a smooth interpolation between the two curves has been sketched in the range of  $P$  near  $P_c$ .

The sample in the experiment appears to exhibit this type of bimodular behaviour. The frequency of the fractured sample increases with load until it has roughly the same frequency as the unbroken sample, which is analogous to going from the open-crack to the closed-crack state. This model can also serve as a simple example of the effect of crack closure under load on the elastic modulus of a body with many microcracks.

## References

1. W. A. ZISMAN, *Proc. Natl. Acad. Sci. USA* **19** (1933) 653.
2. B. T. KELLY, "Physics of Graphite" (Applied Science, London, 1981) p. 98.
3. E. D. CASE, *J. Mater. Sci.* **19** (1984) 3702.
4. B. BUDIANSKY and R. J. O'CONNELL, *Int. J. Solids Struct.* **12** (1976) 81.
5. D. P. H. HASSELMAN, "Tables for the Computation of Shear Modulus and Young's Modulus of Rectangular Prisms" (Carborundum Co., Niagara Falls, New York, 1961).
6. G. PICKETT, *ASTM Proc.* **45** (1945) 846.
7. S. SPINNER and W. E. TEFFT, *ibid.* **61** (1961) 1221.
8. S. TIMOSHENKO, D. H. YOUNG and W. WEAVER, "Vibration Problems in Engineering" 4th Edn (Wiley, New York, 1974) p. 455.
9. J. P. DEN HARTOG, "Strength of Materials" (Dover, New York, 1961) p. 205.

Received 8 August  
and accepted 23 September 1986